

RobotFingerPrint: Unified Gripper Coordinate Space for Multi-Gripper Grasp Synthesis

Ninad Khargonkar, Luis Felipe Casas, Balakrishnan Prabhakaran, Yu Xiang

Abstract—We introduce a novel representation named as the **unified gripper coordinate space** for grasp synthesis of multiple grippers. The space is a 2D surface of a sphere in 3D using longitude and latitude as its coordinates, and it is shared for all robotic grippers. We propose a new algorithm to map the palm surface of a gripper into the unified gripper coordinate space, and design a conditional variational autoencoder to predict the unified gripper coordinates given an input object. The predicted unified gripper coordinates establish correspondences between the gripper and the object, which can be used in an optimization problem to solve the grasp pose and the finger joints for grasp synthesis. We demonstrate that using the unified gripper coordinate space improves the success rate and diversity in the grasp synthesis of multiple grippers.¹

I. INTRODUCTION

Grasp planning or grasp synthesis is an important problem in robotics. Traditional grasp planners such as GraspIt! [1] and OpenRAVE grasp planner [2] adopt a sampling and evaluation strategy, in which the grasps are sampled around an object and the force closure analysis [3] is utilized to evaluate the grasps sampled. These grasp planners are usually computationally expensive and may require users to specify contact points on the grippers. Recently, learning-based grasp synthesis has received more attention. These methods use generative machine learning models such as variational autoencoders [4], [5] or diffusion models [6] for grasp synthesis. These models are trained on large-scale datasets of grasps with various objects [7], [5], [8]. Therefore, they can predict grasps for unseen objects. However, most learning-based models are only trained for a specific gripper such as the Franka Panda gripper [4], [9] or a five-finger gripper [10]. Consequently, these models cannot support multiple grippers or be used for new grippers outside the training domain.

In order to train a single grasp synthesis model to support multiple grippers, researchers have explored predicting some intermediate representations of grasps, instead of directly predicting grasp pose and joint values which are specific for each gripper. In the literature, two types of intermediate representations of grasps have been explored: *gripper keypoints* and *contact maps*. For example, UniGrasp [11] and GeoMatch [12] train neural networks to predict the locations of gripper keypoints on an input object and then solve inverse kinematics to obtain the grasps. GenDexGrasp [13] predicts the contact map of a given object and then solves

All authors are affiliated with the Department of Computer Science, University of Texas at Dallas, Richardson, TX 75080, USA {ninadarun.khargonkar, luis.casasmurillo, bprabhakaran, yu.xiang}@utdallas.edu

¹Project page is available at: <https://irvlutd.github.io/RobotFingerPrint>

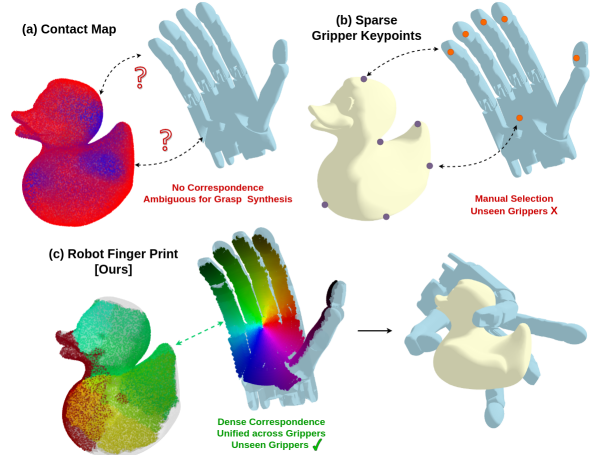


Fig. 1: Comparison between three different representations for grasp synthesis: (a) contact map; (b) sparse gripper keypoints; (c) our unified gripper coordinate space

an optimization problem to generate grasps that comply with the contact map. These intermediate representations can be used with different grippers, even for unseen grippers outside the training domain.

We notice that both gripper keypoints and contact maps have limitations in grasp synthesis. First, gripper keypoints are sparse, i.e., usually a few keypoints are sampled on the gripper. Therefore, noises at keypoint locations can significantly affect grasp quality. In GeoMatch [12], users have to manually specify these keypoints. Second, contact maps are ambiguous for grasp synthesis and their order has to be pre-determined. They provide only information about the distances between the grippers and the objects, but there is no information about how each finger should touch the object.

In this work, motivated by the normalized object coordinate space in object pose estimation [14] and the dense human pose estimation [15] from the computer vision community, we introduce a novel intermediate representation of grasps named the *Unified Gripper Coordinate Space (UGCS)*. This space is the two-dimensional surface of a sphere in the three-dimensional space denoted S^2 . The coordinates in this space are longitude $\lambda \in [-\pi, \pi)$ and latitude $\varphi \in [-\frac{\pi}{2}, \frac{\pi}{2})$. This space is shared among any robotic gripper. Given a gripper, we propose an algorithm to map the inner surface of the gripper, i.e., “palm” of the gripper, into UGCS. Therefore, every 3D point on the palm is assigned a 2D coordinate (λ, φ) . We consider these points as the “finger print” of the robotic gripper. In order to synthesize grasps, we train a conditional variational autoencoder (CVAE) to

map a latent vector and a point cloud of an object to the unified gripper coordinate space. Specifically, CVAE predicts a unified gripper coordinate (λ, φ) for every point on the surface of the object. Using the predicted unified gripper coordinates, a correspondence is established between the object surface and the gripper palm. Then we solve an optimization problem using the predicted unified gripper coordinates to obtain the grasp pose and the finger joint values of a grasp.

Compared to using gripper keypoints or contact maps for grasp synthesis, our proposed UGCS establishes dense correspondences between a gripper and an object, which is robust to noises in the CVAE predictions and resolves the ambiguities from contact maps. In addition, since the UGCS is shared among all grippers, it enables grasp transfer between grippers. We conducted grasp synthesis experiments using the MultiDex dataset [5]. Our method, RobotFingerPrint, outperforms GenDexGrasp [5] and GeoMatch [12] in terms of grasp success rate and grasp diversity.

II. RELATED WORK

A. Analytic Grasp Synthesis

Classic grasp planners such as GraspIt! [1] and OpenRAVE grasp planner [2] use analytic approaches to access grasp quality. Such methods employ task wrench space analysis [16], [17] or force closure analysis [3], [18] to assess the feasibility of a proposed grasp. These traditional grasp synthesis methods usually use sampling-based optimization algorithms, such as simulated annealing to sample grasps, and then evaluate them, which makes the optimization quite slow. Some methods also require the user to manually specify the preferred contact regions on the gripper surface prior to starting the grasp generation process. Recent analytic grasp synthesis leverages Differentiable Force Closure (DFC) [19] in grasp optimization, where the optimization runtime is significantly improved. The main limitation of analytic methods is that the success rate of grasping may not be guaranteed. Because force closure analysis cannot account for other factors in grasping such as friction, materials of objects, noises in control, etc.

B. Learning-based Grasp Synthesis

To improve speed and success in grasp synthesis, more efforts have recently been devoted to learning-based grasp synthesis. Datasets of grasps are first constructed for learning. These grasps are then verified as successful in a physics simulator. Representative datasets include Acronym [7], UniGrasp [11], DexGraspNet [20], Fast-Grasp'D [8], GenDexGrasp [13] and MultiGripperGrasp [21]. These datasets contain different numbers of grippers, objects, and grasps, which can be used to learn generative models for grasp synthesis such as variational auto-encoders or diffusion models.

Grasp synthesis for a single gripper. Most learning-based methods can only plan grasps for a specific type of robotic gripper. For example, [4], [22], [9] deal with parallel

jaw grippers while FFHNet [10] is designed for a five-finger gripper. Unlike analytic approaches, these learning-based methods cannot plan grasps for a variety of robotic grippers.

Grasp synthesis for multiple grippers. Recently, a few approaches are proposed for grasp synthesis of multiple grippers. AdaGrasp [23] uses gripper features to convolve with scene features to generate grasps. UniGrasp [11] trains a neural network to predict finger-tip contact points on objects and then solves inverse kinematics to generate grasps. However, both AdaGrasp and UniGrasp cannot scale-up to grippers with more than 3 fingers. GenDexGrasp [13] trains a conditional variational autoencoder to predict contact map of a given object and then solves an optimization problem using the predicted contact map to generate a grasp. GeoMatch [12] follows a similar idea as UniGrasp [11] to predict keypoints of grippers on object surfaces and then solve inverse kinematics to compute grasps. Different from existing methods, we introduce a novel contact map representation that encodes dense correspondences of gripper surface and object surface. This representation improves success rate and diversity in multi-gripper grasp synthesis across several scenarios.

III. METHOD

A. Unified Gripper Coordinate Space (UGCS)

The Unified Gripper Coordinate Space (UGCS) is a coordinate space that represents the points on the interior surface of a gripper by mapping them onto the surface of a sphere. This coordinate space is common to different grippers and provides a dense representation of the interior surface. A sphere was chosen because of its smooth surface point representation and the fact that similar contact regions can be marked unambiguously across grippers with varying scales. The UGCS representation assigns a normalized coordinate (λ, φ) , with each component in $[0, 1]$ obtained after normalizing the longitude and latitude in their ranges $\lambda \in [-\pi, \pi)$ and $\varphi \in [-\frac{\pi}{2}, \frac{\pi}{2})$. Next, we present the method for constructing such a unified coordinate space across different grippers via their grasps on an associated maximal sphere.

1) *Maximal Sphere Computation:* Since the geometry and kinematics amongst grippers differ significantly, there is no single sphere that can be used to assign this coordinate mapping. Hence, we first created a test bed in simulation to obtain the maximal graspable sphere for each gripper, and used it to assign the coordinate mapping. We used Nvidia's Isaac Sim [24] robotic simulator based on the MultiGripperGrasp [21] toolkit. The simulation consisted of top-down grasps of spheres with increasing radii. These spheres were initialized with their pole touching the gripper palm, and the position, joint values of the gripper at the moment of contact were recorded. Each grasp is simulated for 3 seconds after gripper comes in contact with the object. A grasp is considered successful if, at the end of the grasp the sphere is still in contact with the gripper. Fig. 3 shows the process of sphere-grasping tests in Isaac Sim. The maximal sphere is then determined by the maximum radius within the subset of successful grasps. The maximal graspable sphere

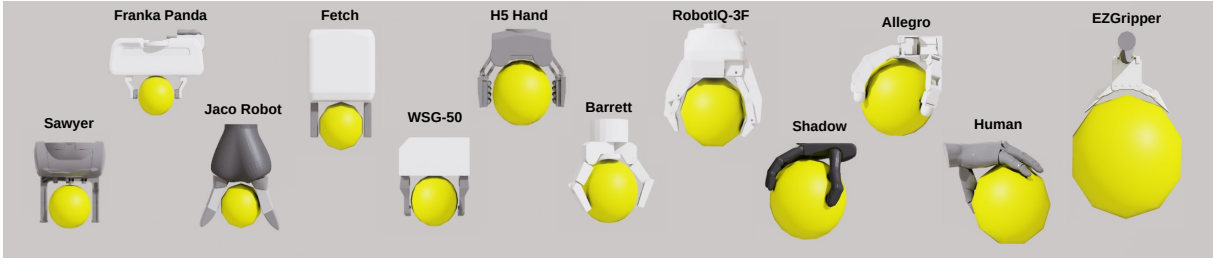


Fig. 2: Max spheres across all the 12 different grippers including the gripper set from MultiGripperGrasp [21] dataset.

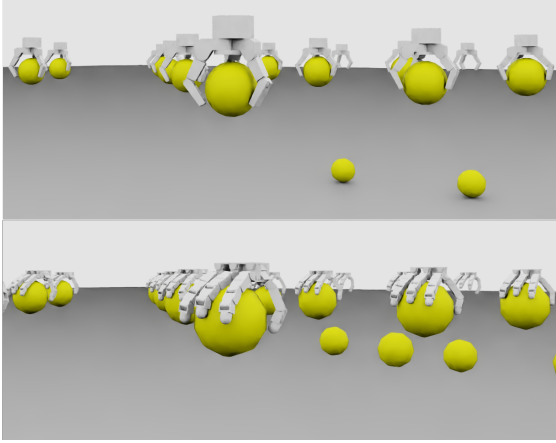


Fig. 3: Maximal Graspable Sphere: We test for multiple spheres with varying radii in parallel via Isaac Sim [24]

of all grippers in the MultiGripperGrasp [21] and MultiDex [5] datasets can be seen in Fig. 2.

2) *UGCS for Gripper Points*: We use the maximal sphere for each gripper to assign a (λ, φ) coordinate to the gripper’s interior surface points. We only consider the interior surface points as they are in contact or close proximity with object for any grasp. This also reduces the ambiguity in which gripper regions are supposed to contact the object, leading to stable grasps. The interior gripper surface points set P_G is computed by uniformly sampling a set R of unit ray directions from the sphere center and checking for ray-mesh intersections $\mathcal{I}_1(\hat{r}, G)$ with the gripper’s meshes.

$$P_G = \{v_g \in G \mid \exists \hat{r} \in R, \text{ s.t. } \mathcal{I}_1(\hat{r}, G) = v_g\}.$$

Each intersecting unit ray direction \hat{r} can alternatively be viewed as surface points on a unit sphere with some spherical coordinate ($radius = 1; \lambda, \varphi$). If the unit ray \hat{r}_g was used to obtain an interior surface point $v_g \in P_G$, then we simply assign the ray’s angular component of the spherical coordinate $(\lambda_{\hat{r}_g}, \varphi_{\hat{r}_g})$ as the gripper point’s coordinate: $(\lambda_{v_g}, \varphi_{v_g}) := (\lambda_{\hat{r}_g}, \varphi_{\hat{r}_g})$. Consequently, with a uniform set of rays, we get dense gripper surface points and their associated coordinates. For M gripper interior surface points, we obtain a UGCS gripper representation with shape $(M, 2)$ and label this as Φ_G . Note that unlike manually selected sparse gripper key points, the UGCS representation is not affected by the ordering of points or the number M . Fig. 4 illustrates the idea behind obtaining Φ_G for each gripper.

B. Grasp Representation

Given a set of grasps on an object with a given gripper, we show how to utilize the UGCS representation with a coordinate map Φ on the object point cloud. Note that the gripper point cloud P_G with its M interior surface points and the corresponding UGCS coordinate map Φ_G are fixed across the different grasps on the object set. Consider an object point cloud O having N points and a grasp for gripper G with its fixed interior surface point set P_G in the object frame. Now, we have N object points and M gripper points in the object frame, with each gripper point having a corresponding (λ, φ) coordinate. For the object’s coordinate map Φ_O , we assign coordinates from the closest gripper point.

$$\Phi_O^{(v_o)} = \Phi_G^{(v_g^*)} \text{ where } v_g^* = \underset{v_g \in P_G}{\operatorname{argmin}} \|v_o - v_g\|.$$

In this way, we obtain a UGCS coordinate for each object point in O . The object map Φ_O provides an alternate grasp representation on the object, and its object-centric form is not constrained by the differences in grippers. A drawback in the above formulation is that it assigns a coordinate (λ, φ) to each object point v_o regardless of its distance to the gripper and without considering whether it is actually in contact or not. In order to represent such no-contact object points in P_O , we simply map them to a default coordinate of $(\lambda = 0, \varphi = 0)$.

Object points with such a coordinate give signal to the learning model that they are not in contact with the object. We can safely assign this specific coordinate as we are guaranteed that no gripper point ever gets assigned this coordinate. This specific coordinate represents the opposite pole of the sphere from where it was grasped. The maximal sphere simulation test ensures that no gripper point gets projected to this coordinate (see Fig. 4). Finally, similar to a contact-map dataset on multi-gripper grasps, we create a coordinate-map dataset with grasps on the objects. Fig. 5 shows some examples of such grasp coordinate maps on object surface with the no-contact regions being transparent.

C. Model Architecture

The overall goal for our RFP method is to synthesize grasps on objects and generalize to unseen grippers and objects. In our modeling setup, we assume that we are given an object point cloud P_O with N points. The prediction problem consists of predicting the intermediate grasp representation of object coordinate map Φ_O with a values (λ, φ) for each of

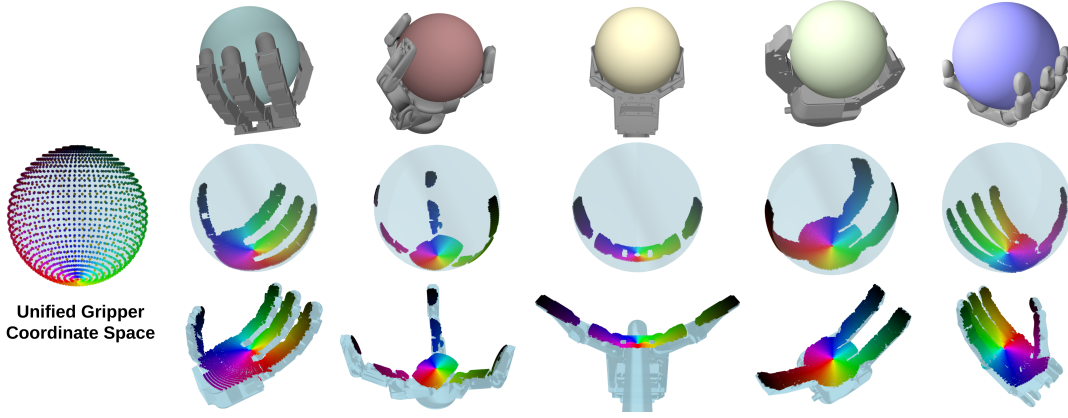


Fig. 4: Visualization of Unified Gripper Coordinate System on grippers from MultiDex [5] and their corresponding sphere points. The colors indicate where each gripper’s region is mapped on the sphere surface.



Fig. 5: Ground-truth coordinate map Φ_O on the object set with some sample grasps from the MultiDex [5] dataset.

the N points. We pose this as a generative modeling problem and utilize the CVAE architecture used in previous works on hand-object grasping [25], [5].

The goal for the learning model is to reason about the grasps on the object O and predict the intermediate grasp representations in the form of object coordinate maps Φ_O . Here each grasp q on O is represented by its associated coordinate map Φ_O . Given P_O and its coordinate map Φ_O , the encoder p_α of the C-VAE model learns to encode the object point cloud and the coordinate map into a latent vector z by modeling the distribution $p_\alpha(z|P_O, \Phi_O)$. The decoder p_β learns to predict an accurate $\hat{\Phi}_O$ on the object given a randomly sampled z by modeling the distribution $p_\beta(\Phi_O|z, P_O)$. We utilize PointNet++ [26] based backbone, where the final output consists of $(\hat{\lambda}, \hat{\varphi})$ coordinate prediction for each point in the object point cloud.

The model is learned by using a standard loss formulation for CVAE with two components for the training objective function. The first component consists of the reconstruction loss L_{recon} on the ground truth coordinate map Φ and its prediction $\hat{\Phi}$: $L_{recon} = \sum_{i=1}^N \|\Phi_O^{(i)} - \hat{\Phi}_O^{(i)}\|$. The second component consists of a KL-divergence term L_{KL} between a prior distribution on the latent space $p_z = \mathcal{N}(0, 1)$ and the approximate posterior modeled by the decoder

$p_\beta(\Phi_O|z, P_O)$: $L_{KL} = D_{KL}(p_z, p_\beta)$. The total loss is a weighted sum between the two: $L_{total} = w_1 L_{recon} + w_2 L_{KL}$. During inference, given an object point cloud, we sample a latent vector $z \sim \mathcal{N}(0, 1)$ and pass it through the decoder along with the point cloud to obtain the predicted coordinate map $\hat{\Phi}_O$. This output is then used as an intermediate representation for grasp optimization on a given gripper as shown in Fig. 6.

D. Grasp Optimization

1) *Coordinate Map Correspondence*: The ultimate goal of the method is to produce a grasp configuration q_G with pose and joint values on an object O and a target gripper G . We generate q_G for a predicted object coordinate map $\hat{\Phi}_O$ and G via a correspondence-driven optimization with the gripper coordinate map Φ_G on its interior surface point set P_G . In contact map based grasp synthesis, the predicted contact map is oblivious to the gripper fingers and hence ambiguous to interpret. A key advantage of UGCS is that we can easily establish a correspondence between an object O with $\hat{\Phi}_O$ and gripper G with Φ_G . Given N object points, and M gripper points, we establish a correspondence between them by assigning each object point v_o to a gripper point $v_g^{*(o)}$ based on the great-circle distance D_H (also known as the Haversine distance) between their respective coordinates $(\hat{\lambda}_{v_o}, \hat{\varphi}_{v_o})$ and $(\lambda_{v_g}, \varphi_{v_g})$. The distance is computed after projecting the coordinates back from the normalized space to the original ranges for latitude and longitude.

$$v_g^{*(o)} = \operatorname{argmin}_{v_g \in P_G} D_H \left((\hat{\lambda}_{v_o}, \hat{\varphi}_{v_o}); (\lambda_{v_g}, \varphi_{v_g}) \right).$$

Using this procedure we obtain a dense mapping between the object and gripper points and it can guide the grasp optimization towards suitable grasps for $\hat{\Phi}_O$. While establishing this correspondence, we do not consider probable no-contact object points which are inferred on the basis of low values for both of their predicted coordinates. The final result from the correspondence are two matching subsets $P_{O_c} \subset O$ and $P_{G_c} \subset P_G$ from the object and gripper points, respectively.

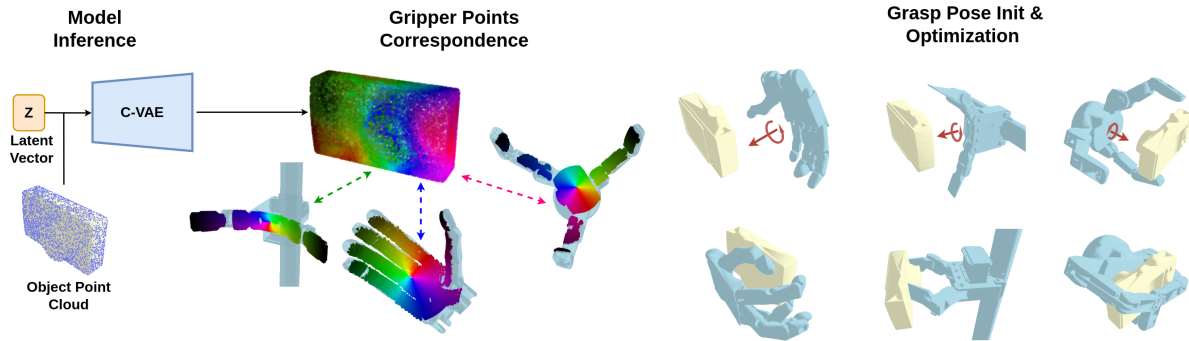


Fig. 6: Method Overview: A randomly sampled latent vector is decoded to a probable object coordinate map $\hat{\Phi}_O$. Given a target (possibly unseen) gripper, correspondence is established between object and gripper points using $\hat{\Phi}_O$. The same $\hat{\Phi}_O$ also guides the pose initialization for the grasp optimization which results in successful grasps.

2) *Pose Initialization*: A possible way to initialize the optimization procedure for q_G would be to sample random gripper poses around the object via some heuristics. However, this can lead to suboptimal grasps due to improper initialization. We observe that in addition to the correspondence, the predicted coordinate map $\hat{\Phi}_O$ contains another signal to the optimization procedure in terms of probable gripper pose. During the construction for UGCS, each of the grippers grasps the sphere with their palm touching the sphere’s south pole with a normalized coordinate value ($\lambda = 0, \varphi = 1$). As a consequence, on the predicted coordinate map $\hat{\Phi}$, we infer a set S_B of probable object points that map to gripper base/palm by thresholding on $\hat{\lambda}$ and $\hat{\varphi}$ using pre-defined thresholds λ_{ub} and φ_{lb} , respectively:

$$S_B = \{v_o \in P_O \text{ s.t. } \hat{\lambda}_{v_o} \leq \lambda_{ub} \text{ and } \hat{\varphi}_{v_o} \geq \varphi_{lb}\}.$$

The initial gripper position is set to $0.1m$ away from the mean of palm-matching set S_B along the mean surface normal for it. The initial gripper 6D pose is determined by aligning the gripper palm normal to the opposite of the mean surface normal from S_B as shown in Fig. 6.

3) *Optimization*: The grasp configuration q_G is obtained by minimizing an objective function that considers hand-object penetration, joint value validity and hand-object distance. A differentiable kinematics model is used to provide gradients on q using the objective function. Note that the hand-object distance is only computed with the corresponding point pairs from P_{O_c} and P_{G_c} . The optimization problem is defined as

$$q_G^* = \underset{q}{\operatorname{argmin}} E_{dist}(P_{O_c}, P_{G_c}; q) + E_{pen}(O, G; q) + E_n(q).$$

The terms for penetration E_{pen} and joint value validity E_n are adopted from [5]. They constrain the grasp q to not collide with the object, and keep the joint values within specified limits. The correspondence-driven E_{dist} acts as a denser version of Inverse Kinematics (IK) by not being limited to only a pre-specified set of sparse keypoints.

IV. EXPERIMENTS

The grasps generated by our method were evaluated using the same simulation protocol used by [5], [12]. Each grasp

is tested for 1 second with 60 simulation steps by applying a consistent acceleration of $0.5m.s^{-2}$ on the object in the NVIDIA Isaac Gym simulation. This process is repeated six times across the positive and negatives axes of the world coordinate frame. A grasp is considered as a failure if the object moves by 2cm at the end of any test. A grasp is labeled as successful if it passes all six tests. We report the same evaluation metrics of grasp success rate and the diversity in successful grasps (standard deviation of the joint values) in order to be consistent with the comparison. The test set comprised of the same split of 10 unseen objects as in [5], [12], and we sampled 64 grasps for each gripper-object pair for evaluation.

A. Grasp Synthesis with Seen Grippers

First, we evaluate the RFP by training with all 5 grippers and evaluating on the test object set. This experiment setting is same as in [12]. We report metrics for Ezgripper, Barrett and Shadowhand as these three grippers have their test results from [5]. Table I shows the success rate and diversity of all the methods using models trained on all the grippers. Results for DFC [19], AdaGrasp [23], GenDexGrasp [5] and GeoMatch [12] are taken from GeoMatch [12]. We observe that RFP outperforms comparable methods in terms of grasp diversity and success rate. Our results are comparable to [12] and better than [5]. It is important to note that while the RFP demonstrates competitive performance with [12], it is capable of dealing with unseen grippers and can generalize well without explicit retraining. Fig. 7 shows some successful grasps from our method.

B. Grasp Synthesis with Unseen Grippers

Furthermore, we compared the performance of our method with that of GenDexGrasp [5] when using out-of-domain grippers and the same test set of unseen objects. The model for an out-of-domain gripper was trained with grasps from all grippers except itself. The comparison is presented in Table II where we see a strong improvement over the prior work across most of the metrics. RFP under-performs GenDexGrasp with ShadowHand in success rate but shows better diversity. It could be due to difficulty in setting up the correspondence for such a dexterous gripper in presence of noisy

TABLE I: Comparison of RFP with prior works on success rate and diversity metrics

Method	Success Rate (%) \uparrow				Diversity (rad) \uparrow			
	ezgripper	barrett	shadowhand	Mean	ezgripper	barrett	shadowhand	Mean
DFC [19]	58.81	85.48	72.86	72.38	0.3095	0.3770	0.3472	0.3446
AdaGrasp [23]	60.00	80.00	-	70.00	0.0003	0.0002	-	0.0003
GenDexGrasp [5]	43.44	71.72	77.03	64.01	0.2380	0.2480	0.2110	0.2323
GeoMatch [12]	75.00	90.00	72.50	79.17	0.1880	0.2490	0.2050	0.2140
RFP (Ours)	72.34	90.00	76.87	79.73	0.2330	0.4240	0.2520	0.3030
RFP* (w/o refinement)	52.5	86.56	55.47	64.84	0.2326	0.4256	0.2519	0.3034

TABLE II: Performance on unseen grippers for RobotFingerPrint (RFP) and GenDexGrasp (GDG) [5]. RFP* represents the experiment with no-refinement ablation.

Gripper	Method	Succ. Rate (%) \uparrow	Diversity (rad) \uparrow
Ezgripper	RFP	63.28	0.224
	RFP*	42.97	0.214
	GDG	38.59	0.248
Barrett	RFP	83.90	0.400
	RFP*	77.96	0.396
	GDG	70.31	0.267
Shadow	RFP	67.96	0.238
	RFP*	51.09	0.238
	GDG	77.19	0.207



Fig. 7: Successful grasps on unseen objects with RFP.

coordinate predictions. On the other hand, RFP outperforms in the case of Ezgripper and Barrett as the correspondence helps the coordinate mapping. With GenDexGrasp, the multi-fingered contact maps from other grippers could induce uncertainty for the finger mapping with Ezgripper or Barrett.

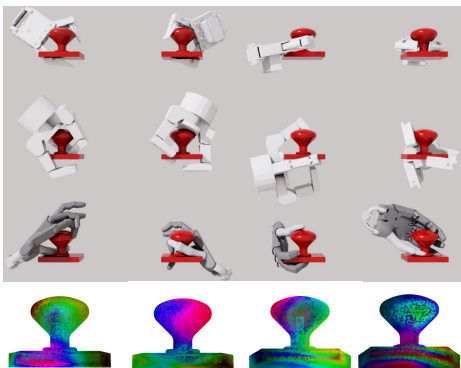


Fig. 8: Similar grasp prediction across different grippers using the same predicted object coordinate map $\hat{\Phi}_O$.

C. Ablation Study: Grasp Refinement in Simulation

We carried out an ablation study for the grasp refinement step used in the simulation evaluation tests as in [5], [12]. A contact-aware refinement is applied to the predicted grasp q via a single gradient update step to obtain force closure around the object. By removing this refinement, we wanted to test the efficacy of our method in terms of its original output. We compare it with the refined outputs from other methods under both in-domain and out-domain settings for the grippers. As seen in Tables I and Table II, RFP without refinement remains competitive even under the removal of this refinement step and establishes strong baselines. It even outperforms on some metrics from prior works [5], [19], [23] which include this refinement during their evaluation. The dense correspondence-driven grasp optimization and a stable pose initialization are able to help the optimization, avoiding bad minima and converging to good quality grasps.

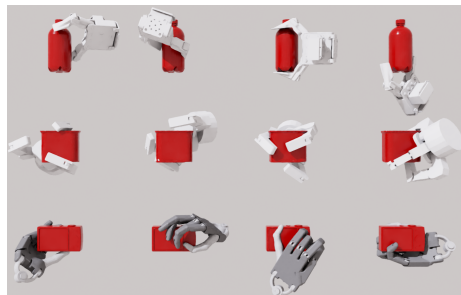


Fig. 9: Failures from the simulation test due to insufficient force closure or not utilizing all the fingers for grasping.

D. Ablation Study: Same Prediction for Different Grippers

Another possible reason for the competitive performance with unseen grippers is visualized in Fig. 8. On the same predicted coordinate map on the object, we observe that the three different grippers grasp the object in similar fashion, especially in terms of approach and position around the object. The mean difference in grasp positions was $0.03m$ for Barrett and Ezgripper while it was around $0.06m$ for both of them with the Shadowhand grasps. This indicates the efficacy of RFP in generalizing the grasps from different grippers in a unified coordinate space. We also present some examples of failure cases in Fig. 9.

V. CONCLUSION AND FUTURE WORK

We introduce RobotFingerPrint (RFP), a novel and effective way to unify grasp representations across differ-

ent grippers into a common coordinate space. The unified grasp representation is dense in nature, requires no manual specification and has an unambiguous mapping to each gripper's individual fingers. Such a mapping helps in synthesizing diverse and stable grasping configurations via a hand-object correspondence and well-initialized grasp optimization which results in strong performance across several evaluation scenarios. We plan to extend the core idea of RFP-driven grasp synthesis to partially observed and incomplete point clouds in real-world grasping scenarios and also utilizing it for grasp transfer from humans. Another avenue of exploration would be to investigate a learned reverse mapping from a coordinate map to grasp prediction without the intermediate grasp optimization.

ACKNOWLEDGMENT

This work was supported by the Sony Research Award Program and the National Science Foundation (NSF) under Grant No. 2346528.

REFERENCES

- [1] A. T. Miller and P. K. Allen, "Grasplit! a versatile simulator for robotic grasping," *IEEE Robotics & Automation Magazine*, vol. 11, no. 4, pp. 110–122, 2004.
- [2] R. Diankov and J. Kuffner, "OpenRAVE: A planning architecture for autonomous robotics," *Robotics Institute, Pittsburgh, PA, Tech. Rep. CMU-RI-TR-08-34*, vol. 79, 2008.
- [3] V.-D. Nguyen, "Constructing force-closure grasps," *The International Journal of Robotics Research*, vol. 7, no. 3, pp. 3–16, 1988.
- [4] A. Mousavian, C. Eppner, and D. Fox, "6-dof graspnet: Variational grasp generation for object manipulation," in *Proceedings of the IEEE/CVF international conference on computer vision*, 2019, pp. 2901–2910.
- [5] P. Li, T. Liu, Y. Li, Y. Zhu, Y. Yang, and S. Huang, "Gendexgrasp: Generalizable dexterous grasping," *arXiv preprint arXiv:2210.00722*, 2022.
- [6] J. Urain, N. Funk, J. Peters, and G. Chalvatzaki, "Se (3)-diffusionfields: Learning smooth cost functions for joint grasp and motion optimization through diffusion," in *2023 IEEE International Conference on Robotics and Automation (ICRA)*. IEEE, 2023, pp. 5923–5930.
- [7] C. Eppner, A. Mousavian, and D. Fox, "Acronym: A large-scale grasp dataset based on simulation," in *IEEE International Conference on Robotics and Automation (ICRA)*, 2021, pp. 6222–6227.
- [8] D. Turpin, T. Zhong, S. Zhang, G. Zhu, J. Liu, R. Singh, E. Heiden, M. Macklin, S. Tsogkas, S. Dickinson *et al.*, "Fast-grasp'd: Dexterous multi-finger grasp generation through differentiable simulation," *arXiv preprint arXiv:2306.08132*, 2023.
- [9] M. Sundermeyer, A. Mousavian, R. Triebel, and D. Fox, "Contact-graspnet: Efficient 6-dof grasp generation in cluttered scenes," in *2021 IEEE International Conference on Robotics and Automation (ICRA)*. IEEE, 2021, pp. 13438–13444.
- [10] V. Mayer, Q. Feng, J. Deng, Y. Shi, Z. Chen, and A. Knoll, "Ffhnet: Generating multi-fingered robotic grasps for unknown objects in real-time," in *2022 International Conference on Robotics and Automation (ICRA)*. IEEE, 2022, pp. 762–769.
- [11] L. Shao, F. Ferreira, M. Jorda, V. Nambiar, J. Luo, E. Solowjow, J. A. Ojea, O. Khatib, and J. Bohg, "Unigrasp: Learning a unified model to grasp with multifingered robotic hands," *IEEE Robotics and Automation Letters*, vol. 5, no. 2, pp. 2286–2293, 2020.
- [12] M. Attarian, M. A. Asif, J. Liu, R. Hari, A. Garg, I. Gilitschenski, and J. Tompson, "Geometry matching for multi-embodiment grasping," in *Proceedings of the 7th Conference on Robot Learning (CoRL)*, 2023.
- [13] P. Li, T. Liu, Y. Li, Y. Geng, Y. Zhu, Y. Yang, and S. Huang, "Gendex-grasp: Generalizable dexterous grasping," in *2023 IEEE International Conference on Robotics and Automation (ICRA)*. IEEE, 2023, pp. 8068–8074.
- [14] H. Wang, S. Sridhar, J. Huang, J. Valentin, S. Song, and L. J. Guibas, "Normalized object coordinate space for category-level 6d object pose and size estimation," in *Proceedings of the IEEE/CVF Conference on Computer Vision and Pattern Recognition*, 2019, pp. 2642–2651.
- [15] R. A. Güler, N. Neverova, and I. Kokkinos, "Densepose: Dense human pose estimation in the wild," in *Proceedings of the IEEE Conference on Computer Vision and Pattern Recognition*, 2018, pp. 7297–7306.
- [16] C. Ferrari and J. F. Canny, "Planning optimal grasps," in *ICRA*, vol. 3, no. 4, 1992, p. 6.
- [17] C. Borst, M. Fischer, and G. Hirzinger, "Grasp planning: How to choose a suitable task wrench space," in *IEEE International Conference on Robotics and Automation, 2004. Proceedings. ICRA'04. 2004*, vol. 1. IEEE, 2004, pp. 319–325.
- [18] D. Berenson and S. S. Srinivasa, "Grasp synthesis in cluttered environments for dexterous hands," in *Humanoids 2008-8th IEEE-RAS International Conference on Humanoid Robots*. IEEE, 2008, pp. 189–196.
- [19] T. Liu, Z. Liu, Z. Jiao, Y. Zhu, and S.-C. Zhu, "Synthesizing diverse and physically stable grasps with arbitrary hand structures using differentiable force closure estimator," *IEEE Robotics and Automation Letters*, vol. 7, no. 1, pp. 470–477, 2021.
- [20] R. Wang, J. Zhang, J. Chen, Y. Xu, P. Li, T. Liu, and H. Wang, "Dexgraspnet: A large-scale robotic dexterous grasp dataset for general objects based on simulation," in *2023 IEEE International Conference on Robotics and Automation (ICRA)*. IEEE, 2023, pp. 11359–11366.
- [21] L. F. Casas, N. Khargonkar, B. Prabhakaran, and Y. Xiang, "Multigrippergrasp: A dataset for robotic grasping from parallel jaw grippers to dexterous hands," 2024. [Online]. Available: <https://arxiv.org/abs/2403.09841>
- [22] H.-S. Fang, C. Wang, M. Gou, and C. Lu, "Graspnet-1billion: A large-scale benchmark for general object grasping," in *Proceedings of the IEEE/CVF conference on computer vision and pattern recognition*, 2020, pp. 11444–11453.
- [23] Z. Xu, B. Qi, S. Agrawal, and S. Song, "Adagrasp: Learning an adaptive gripper-aware grasping policy," in *2021 IEEE International Conference on Robotics and Automation (ICRA)*. IEEE, 2021, pp. 4620–4626.
- [24] NVIDIA, "Nvidia isaac sim: Robotics simulation and synthetic data," 2023. [Online]. Available: <https://developer.nvidia.com/isaac-sim>
- [25] H. Jiang, S. Liu, J. Wang, and X. Wang, "Hand-object contact consistency reasoning for human grasps generation," in *Proceedings of the IEEE/CVF international conference on computer vision*, 2021, pp. 11107–11116.
- [26] C. R. Qi, L. Yi, H. Su, and L. J. Guibas, "Pointnet++: Deep hierarchical feature learning on point sets in a metric space," *Advances in neural information processing systems*, vol. 30, 2017.